THE JOURNAL OF BIOLOGICAL CHEMISTRY VOL. 288, NO. 41, pp. 29494–29505, October 11, 2013

Inflammatory Cytokines Induce a Unique Mineralizing Phenotype in Mesenchymal Stem Cells Derived from Human Bone Marrow*

Received for publication, March 21, 2013, and in revised form, August 2, 2013 Published, JBC Papers in Press, August 22, 2013, DOI 10.1074/jbc.M113.471268

Elisabeth Ferreira[‡§], Ryan M. Porter[‡§], Nathalie Wehling[¶], Regina P. O'Sullivan[‡], Fangjun Liu[‡], Adele Boskey[‖], Daniel M. Estok[**], Mitchell B. Harris[**], Mark S. Vrahas[§‡‡], Christopher H. Evans[‡§1], and James W. Wells[‡§]

From the [‡]Center for Advanced Orthopaedic Studies, Beth Israel Deaconess Medical Center, Boston, Massachusetts 02215, [§]Collaborative Research Center, AO Foundation, 7270 Davos, Switzerland, [¶]Department of Surgery, Asklepios Stadtklinik, 83646 Bad Tölz, Germany, [‖]Hospital for Special Surgery, New York, New York, 10021, [**]Department of Orthopaedic Surgery, Brigham and Women's Hospital, Boston, Massachusetts 02115, and the [‡‡]Department of Orthopaedic Surgery, Massachusetts General Hospital, Boston, Massachusetts 02114

Background: The effects of inflammation upon the biology of human mesenchymal stem cells are poorly understood.
Results: IL-1β provoked massive hydroxyapatite deposition by inhibiting ectonucleotide pyrophosphatase. Cells did not express typical markers of osteoblasts or other mesenchymal lineages.
Conclusion: Inflammation promotes mineralization by a novel mechanism.
Significance: These data provide new insights into cytokine effects on mineralization of soft tissues.

Bone marrow contains mesenchymal stem cells (MSCs) that can differentiate along multiple mesenchymal lineages. In this capacity they are thought to be important in the intrinsic turnover and repair of connective tissues while also serving as a basis for tissue engineering and regenerative medicine. However, little is known of the biological responses of human MSCs to inflammatory conditions. When cultured with IL-1β, marrow-derived MSCs from 8 of 10 human subjects deposited copious hydroxyapatite, in which authenticity was confirmed by Fourier transform infrared spectroscopy. Transmission electron microscopy revealed the production of fine needles of hydroxyapatite in conjunction with matrix vesicles. Alkaline phosphatase activity did not increase in response to inflammatory mediators, but PP_i production fell, reflecting lower ectonucleotide pyrophosphatase activity in cells and matrix vesicles. Because PP_i is the major physiological inhibitor of mineralization, its decline generated permissive conditions for hydroxyapatite formation. This is in contrast to MSCs treated with dexamethasone, where PP_i levels did not fall and mineralization was fuelled by a large and rapid increase in alkaline phosphatase activity. Bone sialoprotein was the only osteoblast marker strongly induced by IL-1β; thus these cells do not become osteoblasts despite depositing abundant mineral. RT-PCR did not detect transcripts indicative of alternative mesenchymal lineages, including chondrocytes, myoblasts, adipocytes, ligament, tendon, or vascular smooth muscle cells. IL-1β phosphorylated multiple MAPKs and activated nuclear factor-κB (NF-κB). Certain inhibitors of MAPK and PI3K, but not NF-κB, prevented mineralization. The findings are of importance to soft tissue mineralization, tissue engineering, and regenerative medicine.

Bone marrow contains populations of mesenchymal stem cells (MSCs)[2] with the ability to differentiate along multiple different mesenchymal lineages (1). As well as contributing to endogenous tissue healing and turnover, MSCs are useful for tissue engineering and regenerative medicine (2). However, the repair site is often inflamed through injury (3) or conditions such as aging, diabetes, obesity, arthritis, and osteoporosis (4); moreover, the surgical implantation of a tissue-engineered construct is likely to provoke iatrogenic inflammation (5). It is thus important to understand the influence of inflammatory mediators on the biology of MSCs.

We previously showed that interleukin-1β (IL-1β) and tumor necrosis factor-α (TNF-α) powerfully inhibit the chondrocytic differentiation of human MSCs (hMSCs) via the transcription factor nuclear factor κB (NF-κB) (6). In subsequent experiments we noted that IL-1β provoked a massive deposition of mineral by hMSCs. This raised the possibility that IL-1β induced the differentiation of the hMSCs into osteoblasts.

Such a conclusion would agree with the recent paper of Sonomoto *et al.* (7). However, Kuroki *et al.* (9) and Gowen *et al.* (8) reported that IL-1β inhibits mineral deposition by human osteoprogenitor cells, and it is well established that IL-1β inhibits the differentiation of rodent osteoprogenitor cells into osteoblasts (10–12).

During osteoblastic differentiation there is sequential expression of genes associated with the osteoblast phenotype (13). Alkaline phosphatase (ALP) is among the first, along with the

* This work was supported, in whole or in part, by National Institutes of Health Grant AR050243 (NIAMS). This work was also supported by AO Foundation Grants S-10-72F and GENDEF.

[1] To whom correspondence should be addressed: Center for Advanced Orthopaedic Studies, BIDMC, RN-115, 330 Brookline Ave., Boston, MA 02215. Tel.: 617-667-4621; Fax: 617-667-7175; E-mail: cevans@bidmc.harvard.edu.

[2] The abbreviations used are: MSC, mesenchymal stem cell; hMSC, human MSC; ALP, alkaline phosphatase; Runx2, runt-related transcription factor 2; ENPP1, ectonucleotide pyrophosphatase/phosphodiesterase 1; MV, matrix vesicles.

TABLE 1
Characteristics of donors used in this study
+ indicates the formation of mineralized matrix in response to the indicated agent. − indicates that no mineralized matrix was formed. The four patients whose cells were studied in greater detail are indicated in bold.

Patient	Gender	Age	Indication	Mineralization response	
				Dex	*IL-1β*
1	Male	78	Femoral neck fracture	+	+
2	Female	76	Femoral neck fracture	+	+
3	Female	81	Femoral neck fracture	+	+
4	**Female**	**71**	**Femoral neck fracture**	**+**	**+**
5	**Male**	**81**	**Dislocated hemiarthroplasty**	**+**	**+**
6	**Female**	**49**	**Posttraumatic arthritis hip**	**+**	**+**
7	Female	31	Infection	+	-
8	Female	51	Posttraumatic arthritis hip	+	-
9	**Male**	**37**	**Posttraumatic arthritis hip**	**+**	**+**
10	male	84	Acetabular malunion	+	+

transcription factors runt-related transcription factor 2 (Runx2) and osterix, followed by the matrix proteins type I collagen, osteopontin, bone sialoprotein, and osteocalcin. Finally, mature osteoblasts deposit a mineralized matrix containing hydroxyapatite. Formation of hydroxyapatite requires inorganic phosphate (P_i), supplied in part by the actions of tissue-nonspecific ALP (EC 3.1.3.1) on suitable substrates. For experimental studies *in vitro*, β-glycerophosphate is usually supplied as the substrate (14).

Mineralization is strongly inhibited by pyrophosphate anions (PP_i) (15), products of several metabolic reactions, particularly those catalyzed by the nucleoside pyrophosphatase phosphodiesterase family of enzymes. The main isoform found in osteoblasts is plasma cell membrane glycoprotein-1 (16), also known as ectonucleotide pyrophosphatase/phosphodiesterase 1 (ENPP1). PP_i is a substrate for ALP, whose actions not only break down this inhibitor of mineralization but also provide P_i for hydroxyapatite formation. The balance between PP_i and P_i is thus a key determinant of mineralization (17, 18).

One primary mechanism of mineralization is thought to be initiated within matrix vesicles (MVs) generated by mineralization competent cells (19, 20). MVs are notably enriched for ENPP1, the sole nucleoside pyrophosphatase phosphodiesterase enzyme present in these structures, and ALP, among other phosphate-generating enzymes (16).

The data described in the present paper show that, although hMSCs deposit abundant mineral in response to IL-1β, they do so without elevating ALP activity. They do not differentiate into osteoblasts or any other of several additional mesenchymal cell types that were assessed. Instead they adopt an unusual phenotype where they mineralize their matrix through an atypical biochemical mechanism.

MATERIALS AND METHODS

Isolation and Expansion of hMSCs—MSCs were isolated from intramedullary reamings collected from 6 female and 4 male patients aged 31–84 years for various orthopedic indications (Table 1) at Brigham and Women's Hospital and Massachusetts General Hospital (Boston, MA). Protocols were approved by all necessary Institutional Review Boards. The stromal fraction of the bone marrow filtrates was isolated by plastic adherence preceded by concentrating nucleated cells either by Ficoll-Paque density gradient centrifugation or by red cell lysis (155 mM NH_4Cl, 10 mM $KHCO_3$, 0.1 mM EDTA, pH 7.2) (21). After 2 weeks in primary culture in low glucose (1 g/dl) Dulbecco's modified Eagle's medium (LG-DMEM, Mediatech, Inc., Manassas, VA) supplemented with 10% fetal bovine serum (FBS; HyClone Laboratories, Inc., Logan, UT) and 1% antibiotic/antimycotic mixture (Invitrogen), cells were passaged and expanded in growth media supplemented with 5 ng/ml FGF-2 (PeproTech, Rocky Hill, NJ) for 2–3 passages. Passage-2 cells were analyzed by flow cytometry for the presence of MSC-associated surface molecules as previously described (21).

Osteoblast Differentiation Cultures—hMSCs were seeded at 5000 cells/cm^2 in LG-DMEM plus 10% FBS. The next day the medium was changed to one containing 50 μg/ml ascorbic acid-2-phosphate (Sigma) supplemented with 100 nM dexamethasone (Sigma), 10 ng/ml rhIL-1β (PeproTech), 10 ng/ml recombinant human TNF-α (PeproTech), or 100 ng/ml rhIL-6/IL-6 soluble receptor (PeproTech). Cultures were supplemented with 10 mM β-glycerophosphate (Sigma) after 10 days of osteogenic culture. In some cultures β-glycerophosphate was replaced by NaH_2PO_4.

Evaluation of in Vitro Mineralization—The presence of calcium-containing deposits was detected by both alizarin red staining and chemical assay. PBS-washed cell layers were fixed for 30 min with 4% paraformaldehyde (Sigma) and stained with 0.5% alizarin red (Sigma) for 5 min. Calcium was extracted from monolayers by incubating overnight in 0.6 N HCl, measured quantitatively as μg/well using a calcium (CPC) Liquicolor kit (Stanbio Laboratory, Boerne, TX). Osteocalcin was quantified using a Mid-Tact human osteocalcin EIA kit (Biomedical Technologies Inc., Stoughton, MA).

Evaluation of Cell Viability—Three assays of cell viability were used: cell adherence, as measured by adherent DNA content, lactate dehydrogenase activity in the medium, and caspase-3/7 activity as a measure of apoptosis. For DNA measurement, PBS-washed adherent cells were trypsinized and resuspended in an equal volume of 2× Tris-buffered solution (20 mM Tris base, 400 mM NaCl, 2 mM EDTA, pH 7.4). Three cycles of freezing-thawing were performed to release DNA, quantified using the Cyquant Cell Proliferation Assay kit (Invitrogen). Lactate dehydrogenase release in culture supernatants was determined using the CytoTox-ONE™ Homogeneous Membrane Integrity Assay (Promega Corp., Madison, WI), and caspase-3/7 activity in cell lysates was quantified using the Apo-ONE® Homogeneous Caspase-3/7 Assay (Promega). Activity was expressed as relative fluorescence units, normalized to DNA content.

Fourier Transform Infrared Spectroscopy (FTIR)—Briefly, 21 days after the addition of dexamethasone or IL-1β to hMSCs in differentiation medium (*i.e.* supplemented with ascorbic acid-2-phosphate and β-glycerophosphate), PBS-washed cell layers were fixed for 30 min with 100% ethanol. Samples were processed as KBr pellets and analyzed by FTIR spectroscopy using established techniques (22). Each spectrum was normalized to the Amide I peak to facilitate comparison of mineral content. Experiments were run in quadruplicate.

ALP Activity—ALP activity was measured colorimetrically using the chromogenic substrate *p*-nitrophenol phosphate. PBS-washed cells were incubated with 1 mg/ml *p*-nitrophenyl

TABLE 2
List and sequences of primers used for analysis of mRNA expression
All sequences are for human genes. F, forward; R, reverse.

Gene	Accession number	Primer sequence 5'-3'	Product size	Primer efficiency
			bp	*%*
18 S rRNA	NR 003286	F: CGGCTACCACATCCAAGGAA R: CGGCTACCACATCCAAGGAA	187	98
ALP	NM 000478	F: CGTGGCTAAGAATGTCATCATGTT R: CGTGGCTAAGAATGTCATCATGTT	90	97
Runx2	NM 001024630	F: GCCTTCAAGGTGGTAGCCC R: CGTTACCCGCCATGACAGTA	67	96
Osteopontin	NM 001040058	F: CCAAGTAAGTCCAACGAAAG R: GGTGATGTCCTCGTCTGTA	348	91
Bone sialoprotein	NM 004967	F: GGCCTGTGCTTTCTCAATGAA R: GCCTGTACTTAAAGACCCCATTTTC	83	87
osterix	NM 152860	F: TGCCCAGTGTCTACACCTCTC R: AGTGTCCCTTGCAGCCCATC	181	100
osteocalcin	NM 199173	F: GTAGTGAAGAGACCCAGGCG R: ATTGAGCTCACACACCTCCC	99	97
Col1A1	NM 000088	F: TGGTTTCGACTTCAGCTTCC R: GAACCACATTGGCATCATCA	92	95

phosphate (Sigma) in 50 mM glycine, 1 mM $MgCl_2$, pH 10.5, at 37 °C for 10 min. ALP activity was calculated from the absorbance at 410 nm of the *p*-nitrophenol reaction product using a microplate reader (SynergyMx, BioTek Instruments, Inc., Winooski, VT). Activity was expressed as nmol of *p*-nitrophenol generated/min, normalized to DNA content. In some experiments cultures were supplemented with 100 μM levamisole (Sigma) for 21 days to inhibit ALP activity.

Pyrophosphate Levels and ENPP1 Activity—PBS-washed cell layers were lysed in 0.1% Triton X-100, 0.2 M Tris-base, 1.6 mM $MgCl_2$, pH 8.1 (23). After three cycles of freezing-thawing, the PP_i content of the cell lysates was quantified using the PiPer™ Pyrophosphate Assay kit (Invitrogen) and expressed as nmol of PP_i/ng of DNA. The 5′-nucleotide phosphodiesterase I assay for ENPP1 was performed colorimetrically using the chromogenic substrate *p*-nitrophenyl-thymidine-5′-monophosphate as previously described (24, 25). 50 μl of cell lysate were incubated with an equal volume of 1 mM thymidine monophosphate *p*-nitrophenyl ester (Sigma) in 50 mM sodium carbonate buffer, pH 9.8, for 1 h at 37 °C. The reaction was stopped by the addition of 4 volumes of 0.1 N NaOH, and the absorbance of the *p*-nitrophenol reaction product was read at 410 nm. ENPP1 activity was expressed as pmol of *p*-nitrophenol formed/h and normalized to DNA content. Experiments were run in quadruplicate.

Isolation and Characterization of Matrix Vesicles—MVs present in the culture medium were harvested from conditioned media. To release matrix-associated MVs, cell layers were incubated with Liberase DH Research Grade (0.14 Wünsch units/ml, Roche Diagnostics) for 30 min at 37 °C. Cell supernatants and Liberase-digested samples were cleared of cells and cellular debris by centrifugation at 20,000 × *g* for 30 min at 4 °C (26). MVs from cleared supernatants were then pelleted by ultracentrifugation at 100,000 × *g* for 60 min at 4 °C (Optima™ TLX Ultracentrifuge; Beckman Coulter Inc., Fullerton, CA). MV pellets resuspended in 400 μl of lysis buffer (250 mM NaCl, 50 mM HEPES, 0.1% Nonidet P-40, pH 7.5) were assayed for protein content using the Pierce® BCA Protein Assay kit (Thermo Scientific, Rockford, IL). PP_i content and ALP and ENPP1 activities were measured as described above. Experiments were run in quadruplicate.

For transmission electron microscopy (EM), monolayers were fixed with 2.5% glutaraldehyde and 2% paraformaldehyde in 0.1 M sodium cacodylate buffer, pH 7.4, at 4 °C overnight. Cells were rinsed in 0.1 M cacodylate buffer and fixed secondarily in 1% osmium tetroxide buffer for 1 h at 4 °C. Water-washed cells were then contrast-fixed in 2% aqueous uranyl acetate for 1 h at 4 °C. Cells were dehydrated in a series of graded ethanols and infiltrated overnight in epoxy resin. Samples were then embedded in epoxy resin and cured at 60 °C for 48 h. Cured blocks were thin-sectioned to 80 nm with a Leica Ultracut E ultramicrotome. Sections were mounted on copper grids and contrast-stained with 2% uranyl acetate for 10 min and lead citrate for 5 min. Sections were observed in Jeol JEM 1400 electron microscope at 120 kV.

Gene Expression—Semiquantitative RT-PCR was used to measure the expression of genes associated with osteogenesis, including ALP, Runx2, osterix, type I collagen (Col1A1), bone sialoprotein, osteopontin, and osteocalcin (Table 2), and to monitor the expression of key marker genes associated with chondrogenesis, tenogenesis, myogenesis, adipogenesis, and vascular smooth muscle cell differentiation (Table 3). Cytoplasmic RNA was extracted from cells using the SV total RNA Isolation System kit (Promega). RNA concentrations were quantified from the absorbance at 260 nm. RNA (1 μg) was reverse-transcribed into cDNA using the GoScript™ Reverse Transcription System kit (Promega) and random primers (0.5 μg). RT-PCR was performed with an Mx3000P™ thermal cycler (Stratagene, Cedar Creek, TX) using either the SYBR® Green Mix kit (Applied Biosystems, Warrington, UK) or the TaqMan® Universal PCR Master Mix kit (Applied Biosystems). For SYBR® Green PCR reactions, the mixture contained 1× SYBR Green, 15-fold diluted cDNA, and 0.2 μM concentrations of each primer. The forward and reverse primers used are listed in Table 2. After 10 min of denaturation at 95 °C, cDNA was amplified in 40 cycles of three steps: 95 °C for 30 s, 55 °C for 60 s, and 72 °C for 30 s. Melting curve analyses were performed at the end of each amplification step. For TaqMan® PCR reactions, the mixture contained 1× Taqman universal PCR Master Mix, 15-fold diluted cDNA, and 1× TaqMan® primer/probe sets. The predesigned real-time PCR primers obtained from Applied Biosystems are listed in Table 3. PCR

TABLE 3
List of the TaqMan® gene expression assays used for analysis of mRNA expression
All primer/probe sets are for human genes.

Gene	Accession number	Assay ID	Amplicon length
			bp
18 S rRNA	X03205.1	Hs99999901_s1	187
Cartilage markers			
Type II collagen	NM_001844.4	Hs00264051_m1	124
Aggrecan core protein	NM_001135.3	Hs00153936_m1	91
Tendon/ligament markers			
Scleraxis	NM_001080514.1	Hs03054634_g1	63
Tenomodulin	NM_022144.2	Hs00223332_m1	73
Muscle markers			
Myogenic differentiation factor 1	NM_002478.4	Hs02330075_g1	87
Myogenic factor 5	NM_005593.2	Hs00929416_g1	114
Vascular smooth muscle cell markers			
α-Smooth muscle actin	NM_001141945.1	Hs00426835_g1	105
Calponin	NM_001033553.2	Hs01060510_m1	74
Adipose tissue markers			
Peroxisome proliferator-activated receptor δ	NM_005037.5	Hs01115513_m1	90
Lipoprotein lipase	NM_000237.2	Hs00173425_m1	103

cycles consisted of 10 min at 95 °C followed by 40 amplification cycles: 95 °C for 15 s and 60 °C for 60 s. The mRNA expression levels were normalized to those of the internal standard 18 S rRNA and reported as relative values (ΔΔCT) to those of the control cells. When required, a relative quantification method using PCR efficiency correction was used as previously described (27). Primer PCR efficiency is documented in Table 2.

Evaluation of Signaling Pathways—To determine a possible role for NF-κB, cells were genetically modified to express a dominant-negative "super-repressor" form of the inhibitor of κB. hMSCs were transduced at subconfluence with up to 5×10^3 viral particles/cell of recombinant adenovirus carrying the super-repressor form of the inhibitor of κB cDNA under the control of the cytomegalovirus immediate-early promoter. The next day cells were reseeded at 5000 cells/cm^2 and maintained in differentiation medium supplemented with dexamethasone or IL-1β for 21 days. NF-κB inhibition was confirmed by co-transducing cells with a NF-κB-responsive luciferase reporter (6) 4 days before analysis of ALP activity and calcium deposition.

Activation of MAPK and Akt pathways was assessed by immunoblotting; 24 h after seeding hMSCs at 10,000 cells/cm^2 in LG-DMEM plus 10% FBS, medium was changed to serum-free medium, and cells were serum-starved for 24 h before adding 10 ng/ml IL-1β. Cells were lysed in buffer (1.5 M Tris, pH 8.8, 0.5 M EDTA, 5 M NaCl, 10% SDS) containing Proteinase Inhibitor Mixture (1:100, Sigma). Lysate protein content was estimated by measuring the absorbance at 280 nm; 20 μg of each sample were resolved by SDS-PAGE on 10% polyacrylamide Ready Gels (Bio-Rad) and electrotransferred onto Immun-Blot® PVDF membranes (Bio-Rad). Blots were blocked using 0.1% Tween 20 and 5% PhosphoBLOCKER™ Blocking Reagent (Cell Biolabs, Inc., San Diego, CA) in Tris-buffered saline, and immunodetection was performed using rabbit primary antibodies and horseradish peroxidase-linked anti-rabbit IgG secondary antibodies (Cell Signaling Technology, Inc., Danvers, MA). Primary antibodies specific for JNK, phospho-JNK, ERK 1/2, phospho-ERK 1/2, p38, phospho-p38, Akt, and phospho-Akt (all from Cell Signaling Technology) were used according to the manufacturer's instructions. Bands were visualized using LumiGLO® reagent (Cell Signaling Technology) on Amersham Biosciences Hyperfilm ECL autoradiography films (GE Healthcare) and a Molecular Imager Gel Doc XR system (Bio-Rad). After initial analysis using phospho-antibodies, blots were stripped using Restore™ Western blot Stripping Buffer (Pierce) and re-probed (once per blot).

The possible roles of MAPK and PI3K in mineralization were evaluated with specific inhibitors that were first screened to identify concentrations that did not affect cell viability, assessed using the CellTiter-Glo® Luminescent Cell Viability Assay (Promega). Cells were seeded at 5000 cells/cm^2 into LG-DMEM with 10% FBS. The next day induction medium supplemented with 2 μM SB203580 or P38-IV (both p38-isoforms α and β- inhibitors), 5 μM PD98059 (MEK1/2 inhibitor) or Erk-II (ERK1/2 inhibitor), 2 μM SP600125 or AS601245 (both JNK-1, -2, -3 inhibitors), or 0.5 μM LY294002 (PI3K inhibitor isoforms α and β) or AS604859 (PI3K inhibitor-isoforms γ) was added to the cells 3 h before culture with 10 ng/ml IL-1β. Alternatively, induction medium was supplemented with inactive analogs of the inhibitors tested: SB202474 for SB203580, U0124 for PD98059, ERK inhibitor II negative control for ERK-II, JNK-II negative control for SP600125, and LY303511 for LY294002. DMSO (0.2%) was used as a control vehicle. All inhibitor molecules were from EMD Biosciences, Inc., La Jolla, CA except AS601245 and AS604859 molecules, purchased from Alexis Biochemicals (San Diego, CA).

Statistical Analysis—Unless otherwise noted, all experiments were run in triplicate using hMSC isolates from 4 to 10 different donors, and representative data sets are shown. Quantitative results are presented as the mean ± S.D. Means were compared using an unpaired, two-tailed Student's *t* test, with *p* values <0.05 considered significant.

RESULTS

Mineralization by hMSCs in Response to Dexamethasone, IL-1β, TNF-α, and IL-6—Cultures were successfully established from each of the 10 donors. Cells recovered in this manner were CD44$^+$, CD90$^+$, CD105$^+$, CD 106$^+$, CD45$^-$, and

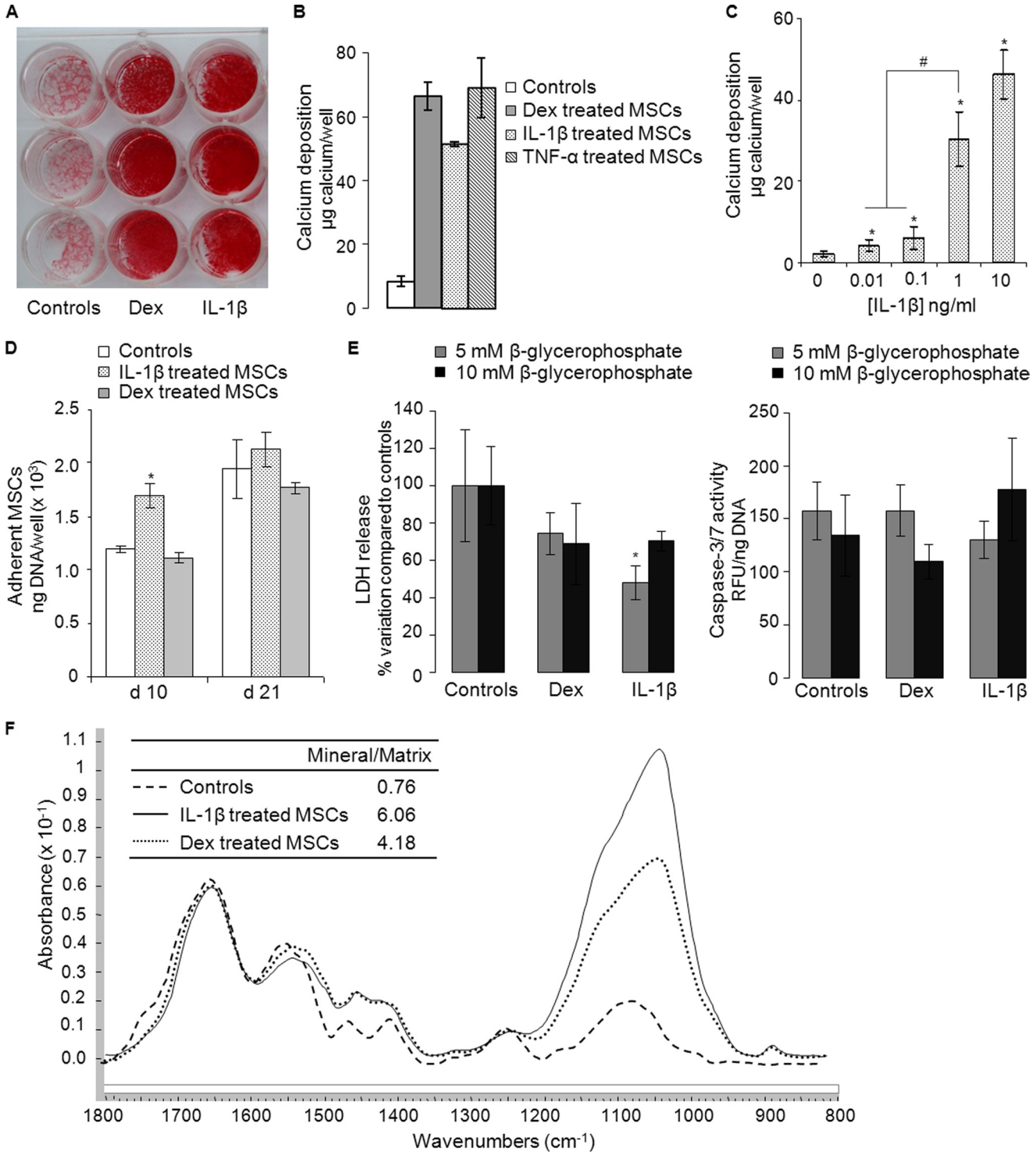

FIGURE 1. ***In vitro* mineralization by hMSCs in response to dexamethasone, IL-1β, or TNF-α and characterization of mineral by Fourier transform infrared spectroscopy.** *A*, alizarin red staining of hMSC monolayers maintained for 21 days in control medium (*Controls*) and medium supplemented with 100 nM dexamethasone (*Dex*) or IL-1β (10 ng/ml). *B*, amount of calcium deposited by hMSCs maintained in medium supplemented with dexamethasone (100 nM), IL-1β (10 ng/ml), or TNF-α (10 ng/ml) for 21 days. C, dose response for the deposition of mineral in response to IL-1β ($n = 3$). * denotes a significant difference ($p < 0.05$) compared with controls lacking IL-1β. # denotes a significant difference ($p < 0.05$) compared with cells treated with 1 ng/ml IL-1β. *D*, hMSC viability, expressed as adherent cell DNA/well, at days 10 and 21 after incubation in medium supplemented with dexamethasone or IL-1β ($n = 3$). * denotes a significant difference ($p < 0.05$) compared with controls. *E*, hMSC death measured as lactate dehydrogenase (*LDH*) release in cell supernatants (*left panel*) and as caspase-3/7 activity in cell lysates (*right panel*). Dexamethasone- and IL-1β-treated cultures were maintained for 21 days in medium supplemented with either 5 or 10 mM β-glycerophosphate ($n = 3$). * denotes a significant difference ($p < 0.05$) compared with controls for a given β-glycerophosphate concentration. *F*, FTIR spectra of matrix formed by hMSC monolayers maintained in basal differentiation medium (*dashed line*) or medium supplemented with dexamethasone (*dotted line*) or IL-1β (*solid line*). All data were normalized to the Amide I peak to facilitate comparison of mineral content. Both dexamethasone-treated cultures and IL-1β-treated cultures showed peaks in the mineral region (900–1200 cm^{-1}).

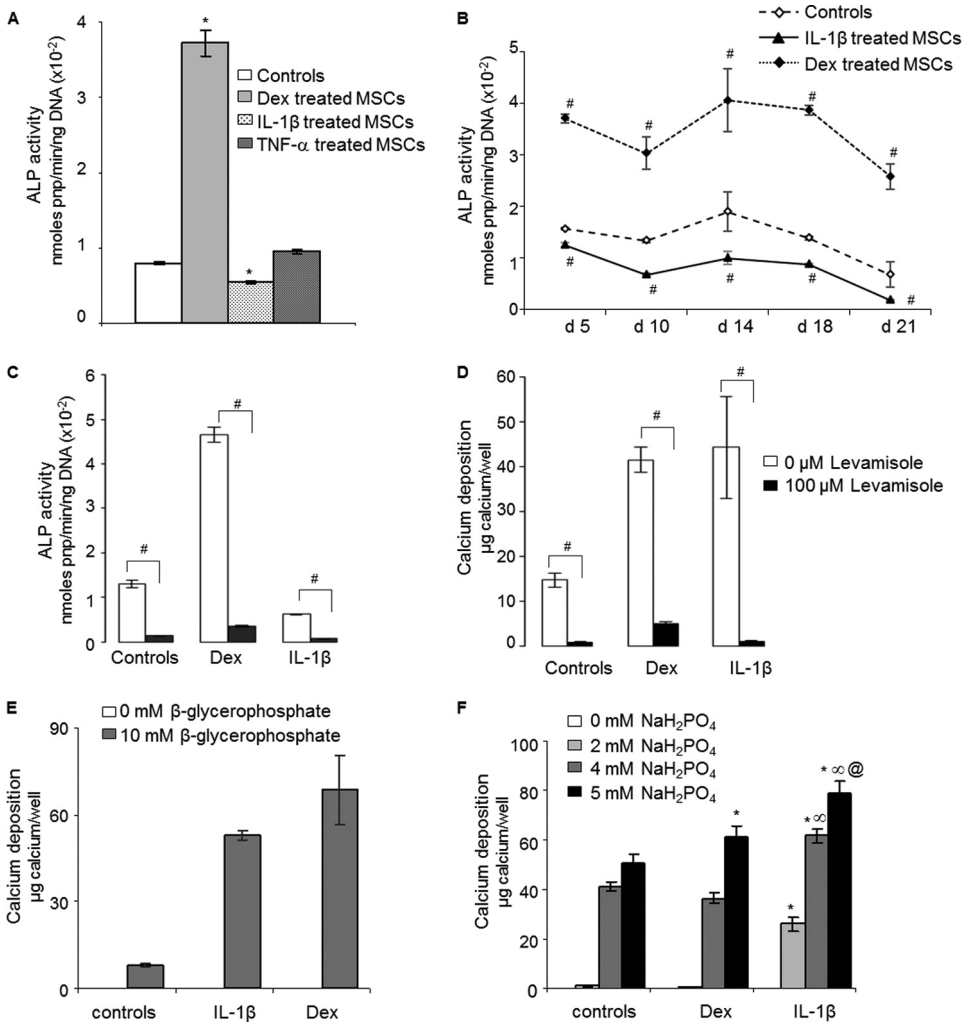

FIGURE 2. **Role of ALP in mineral deposition by hMSCs.** *A*, ALP activity 10 days after incubation in control medium and in medium supplemented with dexamethasone (*Dex*, 100 nM), IL-1β (10 ng/ml), or TNF-α (10 ng/ml) ($n = 3$). * denotes a significant difference ($p < 0.05$) compared with controls. *B*, kinetics of hMSC ALP activity at days 5, 10, 14, 18, and 21 after treatment with dexamethasone or IL-1β. # denotes a significant difference ($p < 0.05$) compared with controls. *C*, inhibition of ALP activity of hMSCs by 100 μM levamisole. # denotes a significant difference ($p < 0.05$) compared with non-levamisole-treated cells. *D*, inhibition by levamisole of calcium deposition by dexamethasone- and IL-1β-treated hMSCs ($n = 3$). # denotes a significant difference ($p < 0.05$) compared with non-levamisole-treated cells. *E*, omission of β-glycerophosphate from the differentiation medium eliminated dexamethasone and IL-1β-induced mineralization ($n = 3$). *F*, effects of increasing concentrations of inorganic phosphate (NaH_2PO_4) on mineral deposition by hMSCs treated with dexamethasone or IL-1β ($n = 3$). * denotes a significant difference ($p < 0.05$) compared with control for each NaH_2PO_4 concentration. ∞ denotes a significant difference ($p < 0.05$) between dexamethasone and IL-1β groups for a given NaH_2PO_4 concentration. @ denotes a significant difference ($p < 0.05$) between 4 and 5 mM NaH_2PO_4 for IL-1β-treated cells.

$CD34^-$ and could differentiate into osteoblasts, chondrocytes, and adipocytes (21). In an initial series of experiments, monolayer cultures of MSCs were maintained for 21 days in the presence of 100 nM dexamethasone or 10 ng/ml IL-1β and stained with alizarin red to assess mineral deposition. All cultures deposited mineral in response to dexamethasone; eight did so in response to IL-1β (Table 1). Such variability is typical of primary, human MSC isolates. Four of the cultures (2 male, 2 female, ages 37–81) that responded to IL-1β were subjected to more detailed analysis.

Deposition of mineral was confirmed qualitatively by alizarin red staining (Fig. 1*A*) and quantitatively by measurement of calcium deposited in the extracellular matrix (Fig. 1*B*); TNF-α (10 ng/ml) also induced mineral deposition (Fig. 1*B*); IL-6/IL-6-soluble receptor (100 ng/ml) did so in 2 of these 4 cultures (data not shown). Dose-response experiments confirmed the sensitivity of hMSCs to IL-1β. A slight increase in mineralization was detected at concentrations as low as 10 pg/ml, whereas robust mineralization occurred at 1 and 10 ng/ml (Fig. 1*C*). A series of experiments in which IL-1β was withdrawn from the medium at various times showed that IL-1β needed to be present for at least the first 10–14 days to induce a mineralization response at 21 days (data not shown). Mineralization in response to dexamethasone was quicker, with mineralized nodules starting to form by 14 days (data not shown). There was no synergy between dexamethasone and IL-1β (data not shown).

DNA measurement of adherent cells indicated that neither IL-1β nor dexamethasone reduced cell viability (Fig. 1*D*). Measurement of lactate dehydrogenase release and caspase 3–7 activity confirmed that neither IL-1β nor dexamethasone induced necrotic or apoptotic cell death (Fig. 1*E*). These observations were not dependent on β-glycerophosphate concentra-

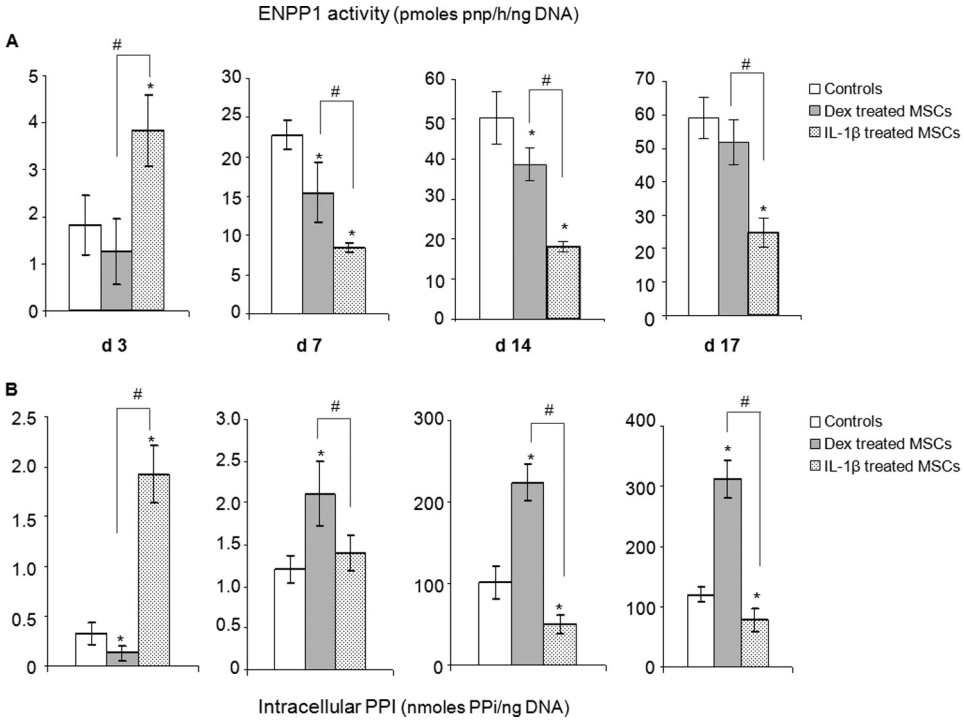

FIGURE 3. **Changes in ENPP1 activity and intracellular PP_i content with time of incubation with dexamethasone and IL-1β.** ENPP1 activity (*A*) and PP_i (*B*) were measured in cell lysates at the indicated times ($n = 4$). * denotes a significant difference ($p < 0.05$) compared with controls (*white bars*). # denotes a significant difference ($p < 0.05$) between dexamethasone (*Dex*, *gray bars*) and IL-1β groups (*dotted bars*). *d*, day.

tion (Fig. 1*E*). Collectively, these results eliminate dystrophic calcification as a trivial explanation of these findings.

For mineral deposited in response to dexamethasone and IL-1β, FTIR analysis provided spectra with broad but strong phosphate peaks at 900–1200 cm^{-1} typical of the poorly crystalline hydroxyapatite found in bone (Fig. 1*F*). The mineral/matrix ratios, which are linearly related to ash content (Fig. 1*F*), indicate that IL-1β and dexamethasone-treated hMSCs had similarly high mineral content.

Role of Alkaline Phosphatase— hMSCs displayed a basal level of ALP activity. Although IL-1β and TNF-α were potent inducers of mineralization, it was not possible to measure an increase in ALP activity for IL-1β- or TNF-α-treated hMSC monolayers and lysates even though a very large increment was noted in response to dexamethasone 10 days after treatment (Fig. 2*A*). A range of additional time points was explored without detecting increased ALP activity in response to IL-1β (Fig. 2*B*). The two cultures that mineralized in response to IL-6/IL-6-soluble receptor also did so without inducing ALP activity (data not shown).

Levamisole, a potent inhibitor of ALP, eliminated both basal and dexamethasone-induced ALP activity (Fig. 2*C*). It completely prevented the deposition of mineral in response to IL-1β and dexamethasone (Fig. 2*D*). Moreover, omission of β-glycerophosphate from the medium eliminated mineralization (Fig. 2*E*). These data suggest that ALP is necessary for mineralization induced by IL-1β even though an increase in this enzyme activity in response to IL-1β was not detected.

In a related series of experiments, β-glycerophosphate was omitted and substituted with NaH_2PO_4 as an alternative and immediate source of phosphate that did not require ALP hydrolysis (Fig. 2*F*). Cells treated with IL-1β, but not those treated with dexamethasone, showed an enhanced ability to deposit a mineralized matrix in response to added phosphate (Fig. 2*E*). This was most evident at a concentration of 2 mM added NaH_2PO_4 (Fig. 2*F*), where cells treated with IL-1β deposited mineral while untreated cells and those treated with dexamethasone did not. This suggests that IL-1β generates an environment that is more conducive to mineralization. We examined the possibility that this reflected a reduction in PP_i.

Role of ENPP1 and PP_i—Cell lysates were assayed for ENPP1 activity and PP_i. ENPP1 activity was strongly increased after 3 days of exposure to IL-1β, whereas dexamethasone had no significant effect (Fig. 3*A*). From day 7 onward, however, there was marked reduction in ENPP1 activity in response to IL-1β. Dexamethasone lowered enzyme activity less dramatically and less persistently.

Intracellular PP_i responded to IL-1β in a fashion that reflected the changing ENPP1 activities, being considerably increased at day 3 and substantially decreased at days 14 and 17 (Fig. 3*B*). When cells were treated with dexamethasone, in contrast, intracellular PP_i was considerably increased from day 7 onward. PP_i was not detectable in the conditioned medium under any conditions of culture (data not shown). Because mineralization by osteoblasts is initiated in MVs that are known to be enriched for ENPP1 and ALP, we isolated these extracellular bodies and measured their ENPP1 and ALP activities as well as their PP_i.

Role of Matrix Vesicles—In agreement with the data obtained with cell lysates (Fig. 3*A*), MVs generated by cells treated with IL-1β had less ENPP1 activity and correspondingly lower PP_i (Fig. 4). MVs generated by cells treated with dexamethasone

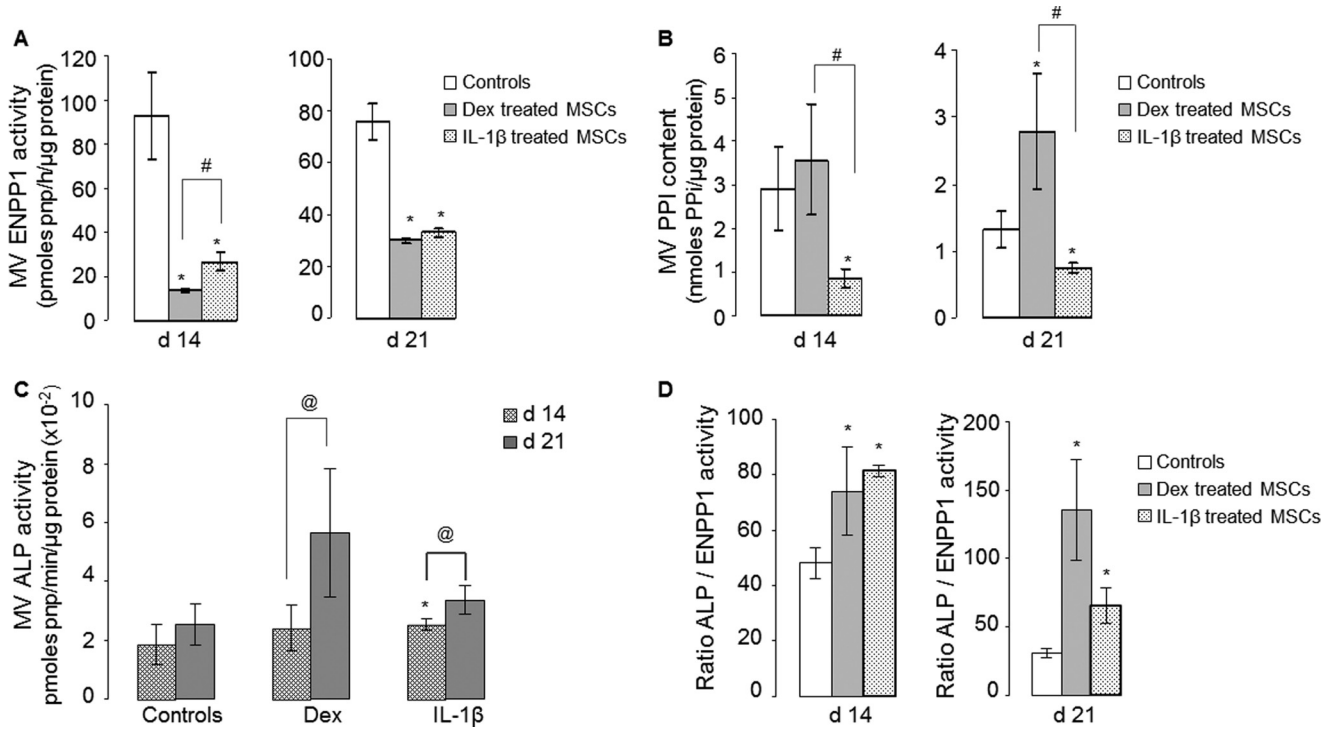

FIGURE 4. **Biochemical properties of matrix vesicles.** MVs were isolated from hMSC cultures 14 and 21 d after treatment with dexamethasone (*gray bars*) or IL-1β (*dotted bars*) ($n = 4$). *A*, ENPP1 activity. *B*, PP_i content. *C*, ALP activity. *D*, ALP/ENPP1 ratios. * denotes a significant difference ($p < 0.05$) compared with controls (*white bars*). # denotes a significant difference ($p < 0.05$) between dexamethasone (*Dex*) and IL-1β groups. @ denotes a significant difference ($p < 0.05$) between 14 and 21-day-old MV lysates for each group tested.

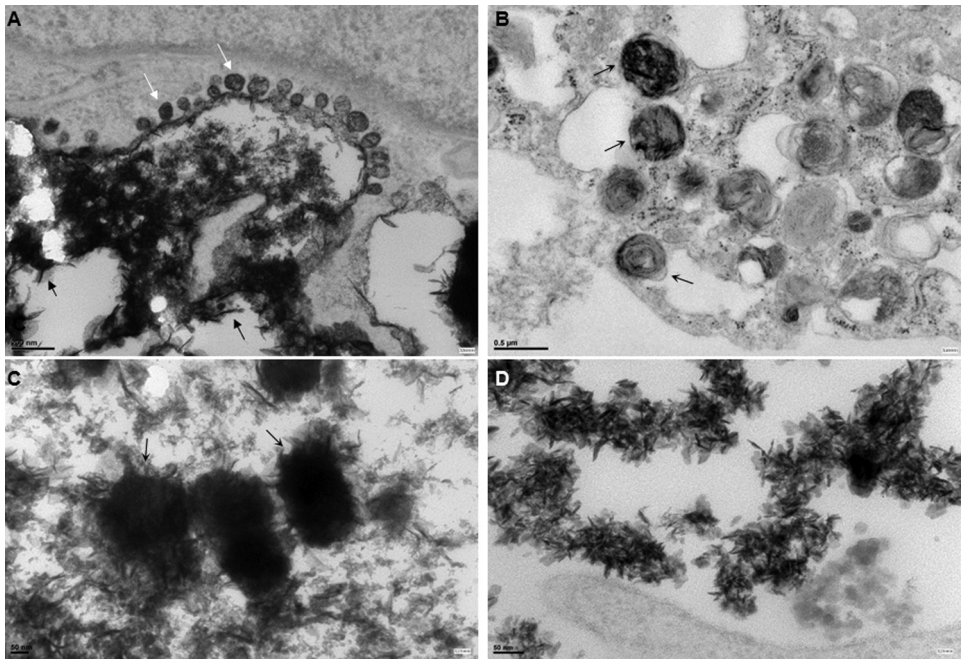

FIGURE 5. **Transmission EM images of hMSCs cultured under different conditions.** *A*, deposition of abundant mineral in region of cell membrane containing membrane-invested vesicles (denoted by *white arrows*) in IL-1β treated hMSCs. *Scale bars*, 200 nm. *Black arrows* show deposits containing fine, needle-shaped crystals typical of hydroxyapatite. *B* and *C*, areas of extracellular matrix of IL-1β-treated cultures containing presumptive matrix vesicles containing mineral (*arrows*). *Scale bars*, 500 and 50 nm, respectively. *D*, needle-shaped crystals of hydroxyapatite were abundant in areas of extracellular matrix of IL-1β-treated cultures. *Scale bar*, 50 nm.

did not follow this pattern; ENPP1 activity was lower (Fig. 4*A*), but PP_i was unchanged at 14 days and increased at 21 days (Fig. 4*B*). At 21 days, ALP activity in MVs (Fig. 4*C*) was increased markedly in response to dexamethasone and modestly in response to IL-1β. Importantly, the ratio of ALP activity to ENPP1 activity was elevated by both dexamethasone and IL-1β, albeit for different reasons (Fig. 4*D*); dexamethasone strongly stimulated ALP activity with a smaller effect on ENPP1, whereas IL-1β had little effect on ALP activity but suppressed ENPP1 activity.

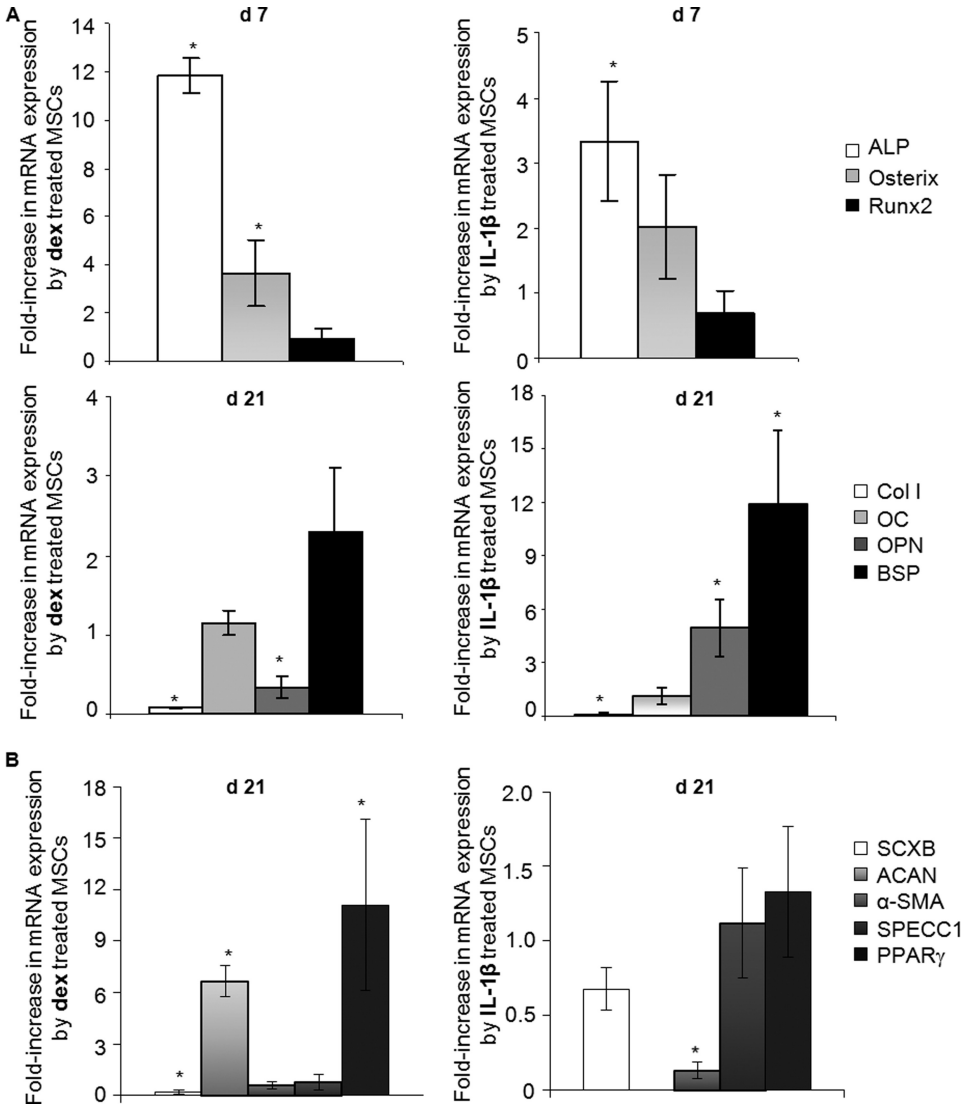

FIGURE 6. **Cell phenotyping by expression of lineage-related transcripts associated with osteoblast, ligament/tendon, chondrocyte, myoblast, vascular smooth muscle cells, and adipocyte.** *A*, mRNA expression of bone-related marker genes. Real time PCR was used to measure the relative expression of early bone-related marker genes including ALP, osterix, and Runx2 (*top panels*) as well as late bone-related marker genes including col1A1 (*Col I*), osteocalcin (*OC*), osteopontin (*OPN*), and bone sialoprotein (*BSP*) (*bottom row*) in cultures treated with dexamethasone or IL-1β ($n = 3$). *B*, mRNA expression of ligament/tendon-related marker, scleraxis (*SCXB*), cartilage-related marker, aggrecan (*ACAN*), vascular smooth muscle cell-related marker genes including α-smooth muscle actin (α-*SMA*) and calponin (*SPECC1*), and fat-related marker, peroxisome proliferator-activated receptor γ (*PPAR*γ) in cultures treated with dexamethasone or IL-1β ($n = 3$). mRNA expression levels were normalized to those of the internal standard 18 S rRNA and are reported as relative values ($\Delta\Delta$CT) to those obtained from the control cell cultures. * denotes a significant difference ($p < 0.05$) compared with controls.

Transmission EM (Fig. 5) confirmed the deposition of mineral aggregates containing fine, needle-shaped crystals consistent with calcium hydroxyapatite. In IL-1β-treated hMSCs, deposition of crystals appeared to be associated with membrane-invested vesicles present at the cell surface (Fig. 5*A*). It was also possible to detect bodies resembling MVs within the ECM (Fig. 5, *B* and *C*), and needle-like crystals of hydroxyapatite were abundantly present in the ECM (Fig. 5*D*). Membrane-invested vesicles were also observed in dexamethasone-treated cultures (data not shown) but were less abundant.

Cell Phenotype—Real-time PCR was used to measure the expression of transcripts associated with the development of the osteoblast phenotype (Fig. 6*A*). Dexamethasone strongly increased ALP mRNA expression and, more modestly, expression of osterix. However, dexamethasone did not up-regulate Runx2, osteocalcin, or bone sialoprotein and inhibited expression of col1A1 and osteopontin. IL-1β slightly increased mRNA expression of ALP and osteopontin, whereas it strongly up-regulated expression of bone sialoprotein transcripts (Fig. 6*A*). However, it had no effect on expression of osterix, Runx2, or osteocalcin and reduced col1A1 expression. ELISA measurements confirmed that osteocalcin protein was not secreted under any conditions of the present study (data not shown).

Real-time PCR was also used to measure the expression of transcripts associated with different mesenchymal lineages including cartilage, ligament/tendon, muscle, vascular smooth muscle, and fat (Fig. 6*B*). Dexamethasone increased aggrecan core protein and peroxisome proliferator-activated receptor γ mRNA expression, inhibited scleraxis expression, and had no effect on the abundance of α-smooth muscle actin and calponin

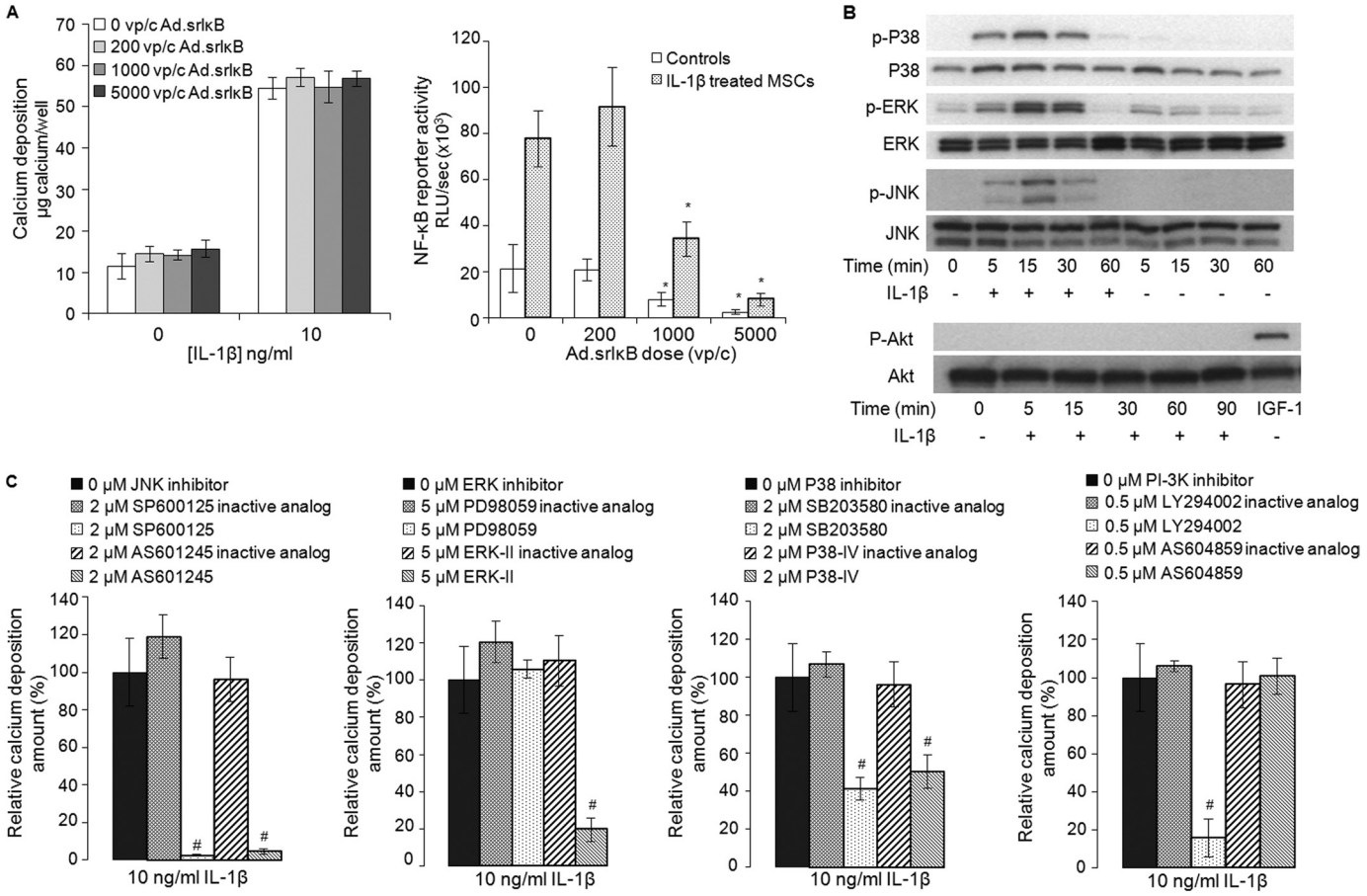

FIGURE 7. **Signal transduction mechanisms involved in IL-1β-mediated mineralization by hMSCs.** *A*, calcium deposition by hMSCs transduced with increasing doses of recombinant adenovirus (*Ad.*) carrying the super-repressor form of the inhibitor of κB (*srIκB*) and exposed to IL-1β for 21 days (*left panel*) and NF-κB inhibition in hMSC cultures transduced with increased doses of Ad.srIκB and treated with IL-1β for 7 days (*right panel*) ($n = 3$). * denotes a significant difference ($p < 0.05$) compared with cells non-transduced cells. *B*, assay of MAPK phosphorylation (p38, ERK, and JNK) and Akt phosphorylation by IL-1β was carried out by Western blot analysis. The blots shown are representative of those obtained in one of 4 experiments ($n = 4$ donors), which each gave similar results. *C*, effect of JNK, ERK, p38, and PI3K inhibitors and their inactive analogs on IL-1β-induced calcium deposition by hMSCs ($n = 3$). Inhibitor molecules were not toxic at the concentrations used. # denotes a significant difference ($p < 0.05$) compared with IL-1β treated cells that were not exposed to inhibitors.

transcripts. IL-1β inhibited expression of α-smooth muscle actin but had no effect on the expression of any other markers (Fig. 6*B*). In addition, mRNA expression of tenomodulin, col2A1, myogenic differentiation factor 1, myogenic factor 5, and lipoprotein lipase was not detected in any of the control or treated cultures (data not shown).

Signal Transduction—Mineralization in response to IL-1β was not inhibited by adenoviral transduction of a dominant-negative super-repressor of NF-κB (Fig. 7*A*), a technique very effective in relieving the inhibition of chondrogenesis by IL-1β in these cells (6). For this reason we focused on the MAPK and PI3K pathways.

Western analysis confirmed that hMSCs respond to IL-1β via p38, ERK, and JNK signaling cascades, but AKT was not phosphorylated (Fig. 7*B*). Specific inhibitors, used to determine which of these were important for mineralization (Fig. 7*C*), were first screened to identify concentrations that did not affect the viability of the cells (data not shown). Non-toxic concentrations of the JNK-specific inhibitors SP600125 and AS-601245 reduced mineralization to a substantial degree. The MEK1/2 inhibitor, PD98059, was only weakly effective, whereas the selective ERK1/2 inhibitor Erk-II strongly inhibited mineralization. Both of the p38-specific inhibitors, SB203580 and P38-IV, also inhibited mineralization. Powerful inhibition was noted with Ly294002, a selective inhibitor of the α, β, and δ isoforms of PI3K, whereas AS604859, which is specific for the γ isoform, had no effect. Inactive analogs of these inhibitors had no effect on mineralization.

DISCUSSION

IL-1β and TNF-α strongly induced mineralization in 8 of 10 cultures of hMSCs. For IL-1β, this was mediated via MAPK and PI3K, rather than NF-κB signaling pathways. Although mineralization required ALP, the addition of IL-1β and TNF-α did not increase its activity, suggesting that the basal levels of ALP expressed by these cells were sufficient. Instead, the major effect of IL-1β was to decrease ENPP1 activity, thereby lowering PP_i, the main physiological inhibitor of mineralization, both in cell lysates and in MVs.

Mineralization in response to dexamethasone occurred by a quite different and more rapid mechanism. The activity of ENPP1 was not affected so dramatically, and PP_i was not reduced in a sustained fashion. Instead, mineralization relied upon a very large and rapid increase in ALP activity. This is the typical mineralization mechanism of most tissues. The mechanism identified in this paper for IL-1β is atypical in that it does

not involve increased alkaline phosphatase activity. Instead the concentration of inhibitory pyrophosphate ions is reduced.

Despite forming MVs and depositing hydroxyapatite, hMSCs did not become true osteoblasts. Expression of Runx2 or osteocalcin was not induced, and in agreement with the work of Diefenderfer *et al.* (28), dexamethasone failed to induce osteopontin or bone sialoprotein, whereas IL-1β did not induce osterix; both agents inhibited expression of col1A1. Moreover, hMSCs treated with IL-1β formed mineral through an atypical mechanism.

Our conclusion disagrees with that of Sonomoto *et al.* (7), but it is hard to determine possible reasons for this discrepancy because they added IL-1β to MSCs in commercial "osteogenic induction medium" that includes dexamethasone and "mesangial cell growth supplement." The presence of dexamethasone would account for the induction of ALP and mineralization, thus obscuring any direct effect that IL-1β might have had. Comparison is further complicated by their use of a commercial MSC line. An intermediate result was published by Ding *et al.* (29) who noted that IL-1β and TNF-α induced mineral deposition by human trabecular bone outgrowth cells by a mechanism involving the induction of ALP but inhibition of RUNX2. Exploration of alternative differentiation pathways for hMSCs treated with IL-1β failed to provide evidence for differentiation into chondrocytes, tenocytes, adipocytes, myocytes, ligament cells, or vascular smooth muscle cells.

Induction of the mineralizing phenotype by IL-1β involved MAPK and PI3K, but not NF-κB pathways. The involvement of PI3K is intriguing. Although the PI3K inhibitor Ly294002 strongly inhibited mineralization in response to IL-1β, we could not detect phosphorylation of AKT, normally a downstream substrate for PI3K. Recent research has identified AKT-independent pathways for PI3K (30), and one such pathway may be operative here. Our inhibitor data suggest this is isoform-specific. The paper by Sonomoto *et al.* (7) emphasizes the role of Wnt signaling in MSC responses to IL-1β, something that was not examined here. These two pathways need not be mutually exclusive; indeed there is growing evidence of Wnt-MAPK synergies in certain cells (31).

It should be noted that IL-1β had a biphasic effect on ENPP1 activity and PP_i (Fig. 3) with an early increase in these parameters by day 3 followed by a protracted decline from day 7 onward. This result is consistent with our observation that IL-1β needs to be present continuously for at least 10–14 days to promote mineralization, and calcium deposits do not form before 15 days. Thus the effects of acute inflammation on hMSC responses could be quite different from the effects of chronic inflammation. The latter is present systemically during aging and in conditions such as obesity, diabetes, rheumatoid arthritis, and osteoporosis (32, 33). Mineralization of soft tissues, such as ligaments and the vasculature, is associated with some of these conditions, and our data suggest one mechanism through which this could occur. With mineralized tissues, the circumstances are more complex because IL-1β and TNF-α not only promote mineralization in the manner described in this paper but also enhance osteoclastogenesis (34).

Much research explores the use of MSCs in the context of tissue engineering and regenerative medicine. Largely ignored is the likelihood that MSCs will need to function in these contexts within an environment that is inflamed as a result of disease, injury, or surgery. The data presented in this paper point to hitherto unappreciated aspects of the biochemical response of hMSCs to inflammation that may influence their ability to promote reparative responses.

Other consequences of the inhibition of ENPP1 by IL-1β are suggested by the progressive mineralization of ligaments and arteries and premature osteoarthritis of mice lacking this enzyme (35). Moreover, humans deficient in ENPP1 develop arterial calcification in infancy associated with periarticular deposits of hydroxyapatite (36).

Acknowledgments—We thank Ann K. Rosenthal and Claudia Gohr, Rheumatology Research, Medical College of Wisconsin, Milwaukee, WI for attempting to measure PP_i in conditioned media. We also thank Hayat Taleb, Hospital for Special Surgery, New York, NY, for performing FTIR analysis, Susan Hagen and Andrea Calhoun, Electron Microscopy Core, Beth Israel Deaconess Medical Center, Boston, MA for performing electron microscopy analysis, and Augustine Rajakumar, Center for Vascular Biology Research, Beth Israel Deaconess Medical Center, Boston, MA for help in processing the samples for ultracentrifugation.

REFERENCES

1. Caplan, A. I., and Dennis, J. E. (2006) Mesenchymal stem cells as trophic mediators. *J. Cell. Biochem.* **98,** 1076–1084
2. Arthur, A., Zannettino, A., and Gronthos, S. (2009) The therapeutic applications of multipotential mesenchymal/stromal stem cells in skeletal tissue repair. *J. Cell. Physiol.* **218,** 237–245
3. Pape, H. C., Marcucio, R., Humphrey, C., Colnot, C., Knobe, M., and Harvey, E. J. (2010) Trauma-induced inflammation and fracture healing. *J. Orthop. Trauma* **24,** 522–525
4. Bastian, O., Pillay, J., Alblas, J., Leenen, L., Koenderman, L., and Blokhuis, T. (2011) Systemic inflammation and fracture healing. *J. Leukoc. Biol.* **89,** 669–673
5. Ni Choileain, N., and Redmond, H. P. (2006) Cell response to surgery. *Arch. Surg.* **141,** 1132–1140
6. Wehling, N., Palmer, G. D., Pilapil, C., Liu, F., Wells, J. W., Müller, P. E., Evans, C. H., and Porter, R. M. (2009) Interleukin-1β and tumor necrosis factor α inhibit chondrogenesis by human mesenchymal stem cells through NF-kappaB-dependent pathways. *Arthritis Rheum.* **60,** 801–812
7. Sonomoto, K., Yamaoka, K., Oshita, K., Fukuyo, S., Zhang, X., Nakano, K., Okada, Y., and Tanaka, Y. (2012) Interleukin-1β induces differentiation of human mesenchymal stem cells into osteoblasts via the Wnt-5a/receptor tyrosine kinase-like orphan receptor 2 pathway. *Arthritis Rheum.* **64,** 3355–3363
8. Gowen, M., MacDonald, B. R., and Russell, R. G. (1988) Actions of recombinant human γ-interferon and tumor necrosis factor α on the proliferation and osteoblastic characteristics of human trabecular bone cells *in vitro*. *Arthritis Rheum.* **31,** 1500–1507
9. Kuroki, T., Shingu, M., Koshihara, Y., and Nobunaga, M. (1994) Effects of cytokines on alkaline phosphatase and osteocalcin production, calcification, and calcium release by human osteoblastic cells. *Br. J. Rheumatol.* **33,** 224–230
10. Gilbert, L., He, X., Farmer, P., Boden, S., Kozlowski, M., Rubin, J., and Nanes, M. S. (2000) Inhibition of osteoblast differentiation by tumor necrosis factor-α. *Endocrinology* **141,** 3956–3964
11. Kaneki, H., Guo, R., Chen, D., Yao, Z., Schwarz, E. M., Zhang, Y. E., Boyce, B. F., and Xing, L. (2006) Tumor necrosis factor promotes Runx2 degradation through up-regulation of Smurf1 and Smurf2 in osteoblasts. *J. Biol. Chem.* **281,** 4326–4333
12. Lacey, D. C., Simmons, P. J., Graves, S. E., and Hamilton, J. A. (2009)

Proinflammatory cytokines inhibit osteogenic differentiation from stem cells. Implications for bone repair during inflammation. *Osteoarthritis Cartilage* **17,** 735–742
13. Murshed, M., Harmey, D., Millán, J. L., McKee, M. D., and Karsenty, G. (2005) Unique coexpression in osteoblasts of broadly expressed genes accounts for the spatial restriction of ECM mineralization to bone. *Genes Dev.* **19,** 1093–1104
14. Bellows, C. G., Heersche, J. N., and Aubin, J. E. (1992) Inorganic phosphate added exogenously or released from β-glycerophosphate initiates mineralization of osteoid nodules *in vitro*. *Bone Miner.* **17,** 15–29
15. Fleisch, H., Russell, R. G., and Straumann, F. (1966) Effect of pyrophosphate on hydroxyapatite and its implications in calcium homeostasis. *Nature* **212,** 901–903
16. Johnson, K. A., Hessle, L., Vaingankar, S., Wennberg, C., Mauro, S., Narisawa, S., Goding, J. W., Sano, K., Millan, J. L., and Terkeltaub, R. (2000) Osteoblast tissue-nonspecific alkaline phosphatase antagonizes and regulates PC-1. *Am. J. Physiol.* **279,** R1365–R1377
17. Hessle, L., Johnson, K. A., Anderson, H. C., Narisawa, S., Sali, A., Goding, J. W., Terkeltaub, R., and Millan, J. L. (2002) Tissue-nonspecific alkaline phosphatase and plasma cell membrane glycoprotein-1 are central antagonistic regulators of bone mineralization. *Proc. Natl. Acad. Sci. U.S.A.* **99,** 9445–9449
18. Johnson, K., and Terkeltaub, R. (2005) Inorganic pyrophosphate (PP_i) in pathologic calcification of articular cartilage. *Front. Biosci.* **10,** 988–997
19. Anderson, H. C. (1995) Molecular biology of matrix vesicles. *Clin. Orthop. Relat. Res.* **314,** 266–280
20. Boskey, A. L. (1992) Mineral-matrix interactions in bone and cartilage. *Clin. Orthop. Relat. Res.* **281,** 244–274
21. Porter, R. M., Liu, F., Pilapil, C., Betz, O. B., Vrahas, M. S., Harris, M. B., and Evans, C. H. (2009) Osteogenic potential of reamer irrigator aspirator (RIA) aspirate collected from patients undergoing hip arthroplasty. *J. Orthop Res.* **27,** 42–49
22. Bonewald, L. F., Harris, S. E., Rosser, J., Dallas, M. R., Dallas, S. L., Camacho, N. P., Boyan, B., and Boskey, A. (2003) von Kossa staining alone is not sufficient to confirm that mineralization *in vitro* represents bone formation. *Calcif. Tissue Int.* **72,** 537–547
23. Harmey, D., Hessle, L., Narisawa, S., Johnson, K. A., Terkeltaub, R., and Millán, J. L. (2004) Concerted regulation of inorganic pyrophosphate and osteopontin by akp2, enpp1, and ank. An integrated model of the pathogenesis of mineralization disorders. *Am. J. Pathol.* **164,** 1199–1209
24. Terkeltaub, R. A., Johnson, K., Rohnow, D., Goomer, R., Burton, D., and Deftos, L. J. (1998) Bone morphogenetic proteins and bFGF exert opposing regulatory effects on PTHrP expression and inorganic pyrophosphate elaboration in immortalized murine endochondral hypertrophic chondrocytes (MCT cells). *J. Bone Miner. Res.* **13,** 931–941
25. Yao, Z., Nakamura, H., Masuko-Hongo, K., Suzuki-Kurokawa, M., Nishioka, K., and Kato, T. (2004) Characterisation of cartilage intermediate layer protein (CILP)-induced arthropathy in mice. *Ann. Rheum. Dis.* **63,** 252–258
26. Xiao, Z., Camalier, C. E., Nagashima, K., Chan, K. C., Lucas, D. A., de la Cruz, M. J., Gignac, M., Lockett, S., Issaq, H. J., Veenstra, T. D., Conrads, T. P., and Beck, G. R., Jr. (2007) Analysis of the extracellular matrix vesicle proteome in mineralizing osteoblasts. *J. Cell. Physiol.* **210,** 325–335
27. Pfaffl, M. W. (2001) A new mathematical model for relative quantification in real-time RT-PCR. *Nucleic Acids Res.* **29,** e45
28. Diefenderfer, D. L., Osyczka, A. M., Garino, J. P., and Leboy, P. S. (2003) Regulation of BMP-induced transcription in cultured human bone marrow stromal cells. *J. Bone Joint Surg. Am.* **85,** 19–28
29. Ding, J., Ghali, O., Lencel, P., Broux, O., Chauveau, C., Devedjian, J. C., Hardouin, P., and Magne, D. (2009) TNF-α and IL-1β inhibit RUNX2 and collagen expression but increase alkaline phosphatase activity and mineralization in human mesenchymal stem cells. *Life Sci.* **84,** 499–504
30. McNamara, C. R., and Degterev, A. (2011) Small-molecule inhibitors of the PI3K signaling network. *Fut. Med. Chem.* **3,** 549–565
31. Guardavaccaro, D., and Clevers, H. (2012) Wnt/β-catenin and MAPK signaling. Allies and enemies in different battlefields. *Sci. Signal.* **5,** pe15
32. Scrivo, R., Vasile, M., Bartosiewicz, I., and Valesini, G. (2011) Inflammation as "common soil" of the multifactorial diseases. *Autoimmun. Rev.* **10,** 369–374
33. Southerland, J. H., Taylor, G. W., Moss, K., Beck, J. D., and Offenbacher, S. (2006) Commonality in chronic inflammatory diseases. Periodontitis, diabetes, and coronary artery disease. *Periodontology 2000* **40,** 130–143
34. Wei, S., Kitaura, H., Zhou, P., Ross, F. P., and Teitelbaum, S. L. (2005) IL-1 mediates TNF-induced osteoclastogenesis. *J. Clin. Invest.* **115,** 282–290
35. Okawa, A., Nakamura, I., Goto, S., Moriya, H., Nakamura, Y., and Ikegawa, S. (1998) Mutation in Npps in a mouse model of ossification of the posterior longitudinal ligament of the spine. *Nat. Genet.* **19,** 271–273
36. Rutsch, F., Vaingankar, S., Johnson, K., Goldfine, I., Maddux, B., Schauerte, P., Kalhoff, H., Sano, K., Boisvert, W. A., Superti-Furga, A., and Terkeltaub, R. (2001) PC-1 nucleoside triphosphate pyrophosphohydrolase deficiency in idiopathic infantile arterial calcification. *Am. J. Pathol.* **158,** 543–554